

EUROPEAN ORGANIZATION FOR NUCLEAR RESEARCH

FC/afm

CERN/PS/85-48 (AA)

PLANAR SLOTLINE PICK-UPS AND KICKERS  
FOR STOCHASTIC COOLING

F. Caspers

Geneva, Switzerland  
August 1985/June 1986

## ABSTRACT

Planar slotline and microstrip configurations on the same dielectric substrate are elements of MICs (Microwave Integrated Circuits). It is proposed to use similar structures for pick-up and kicker applications for stochastic cooling. In this case slotlines on a metallized ceramic substrate ( $\text{Al}_2\text{O}_3$ ) are positioned at a given distance from the beam with their axis transversely or at a fixed angle to the image current. The slotlines may be terminated by slotline-microstrip transitions for further combination of the output signals with a microstrip combiner board. Assuming matched transitions, only travelling waves, launched by the image current (Pick-up) occur in the slotlines (Transverse Travelling Wave Structure, TTWS). It seems that in this case, for a single slotline, a high bandwidth (decade) together with good sensitivity can be achieved. An interesting aspect which should be pointed out is that for TTWS of this kind, the sample slice of the beam is tilted and the tilt angle is determined by the propagation constant of the slotline and its orientation relative to the beam. For narrow bandwidth (octave) a transverse standing wave structure (TSWS) might be more effective since higher sensitivities may be obtained. For slotline arrays the lateral distance between the slots is limited by mutual coupling. The frequency range of application is between ca 100 MHz and 30 GHz using present technology on alumina substrates.

### 1. INTRODUCTION

For pick-up and kicker applications in the GHz range stripline directional couplers or loop structures are widely used. These devices give a high beam coupling impedance over a frequency range of about one octave and can be operated both in the sum and difference modes. Nevertheless, their mechanical construction becomes difficult (microscopic) towards frequencies higher than, say 5 GHz. Therefore, at high frequencies slot pick-ups consisting of a metal plate with an array of slots transverse to the image current are preferred<sup>1</sup>. They exhibit a bandwidth similar to loop pick-ups (resonance of slots) but generally have a lower beam coupling impedance per unit length, their mechanical problems being less severe than those of loop pick-ups. Waveguide-type structures, such as Cerenkov pick-ups and corrugated wall pick-ups have been built, and show a good performance, but have rather small apertures for high sensitivities.

It is the purpose of this paper to discuss a new type of construction consisting of slotlines transverse to the beam (not to be confounded with transverse slots = Faltin<sup>1</sup> type pick-up<sup>1</sup>). The slot pick-up of Faltin may be described as a line propagating a TEM-like wave in the beam direction coupled to the beam by slots in the outer conductor. In contrast to this the slotline pick-up to be discussed here propagates a beam-excited TEM-like wave along a slot between conducting planes perpendicular to the beam direction. The main advantage should be the rather simple fabrication process (double layer planar structure) and thus very well defined mechanical tolerances. Also due to the photolithographic process very small structures and thus high frequencies can be reached.

### 2. PROPERTIES OF SLOTLINES

For a practical approach some aspects of present slotline technology shall be discussed now. Of course, slotlines may be realized as a simple slit in a metal plate. But most slotline applications make use of the dielectric properties of some low loss dielectric material (e.g.  $\text{Al}_2\text{O}_3$ ). The reason is that slotlines are seldom the only element in a

circuit (MIC = Microwave Integrated Circuit), but allow some interesting and elegant solutions in conjunction with microstrips. Since alumina is a very widespread microwave substrate material and also often chosen for accelerator applications (low outgassing, radiation hardness, low electrical loss, mechanical strength) in the following mostly slotlines on alumina are considered. Figure 1 gives an idea of the field and current distributions of a slotline on  $\text{Al}_2\text{O}_3$  substrate. Substantial transverse current densities might occur (Fig. 1c) and formally the E-field across the gap can be replaced by a magnetic current (Fig. 1d). Slotlines are the dual structures to microstrip lines (electric currents - magnetic currents). Note that the coordinate system used in Figs. 1 - 7 is different from that employed in eqs. (1)...(5). Figure 2 shows the influence of the substrate permittivity on the lateral decay of the fields. The dielectric material tends to concentrate the electromagnetic energy close to the gap thus reducing the lateral field spread but also lowering the characteristic impedance and propagation velocity. But with increasing dielectric constant the coupling to an adjacent slotline at a given distance will be reduced. For a fixed coupling the lateral distance decreases. Figures 3 and 4 give an idea about the practical limitations of  $Z_L$  and  $\epsilon_{r,eff}$  and also about the dispersion. For the case depicted here the frequency range is between 200 MHz and more than 15 GHz. With special thin alumina substrates the upper limit can be pushed above 30 GHz (also for microstrip). Using quartz substrates, microstrip circuits for more than 100 GHz have been realized, but quartz is much more brittle than alumina and may cause outgassing problems. The lower frequency limit may be below 100 MHz, if sufficient surface is provided. In contrast to microstrip lines the dispersion is considerably higher, which is due to the fact that for increasing frequency the energy of the slotline wave is being concentrated towards the near vicinity of the slot (Fig. 2). Broadband well-matched microstrip-slotline or coaxial cable-slotline transitions are an essential element of microwave integrated circuits (Fig. 5). They are also limiting the relative bandwidth to about one decade. The spiral configuration in Fig. 5 is reported to have a VSWR less than 1.1 in the 1-10 GHz frequency range.

Another limiting effect for pick-up and kicker applications is the mutual coupling of slotlines (Fig. 6). If more than one slotline is needed, the question arises about the minimum lateral spacing to obtain a given beam coupling impedance per unit length. Coupled slotlines can be treated theoretically as a directional coupler. To describe a directional coupler one needs the odd - and even - mode impedance and the odd - and even - mode phase velocities (Fig. 6b). Another name for two coupled slotlines is the "Coplanar Wave Guide" (Fig. 7). Using coplanar wave guide data is a means for checking the odd-mode coupled slotline results.

A comparison of practical  $Z_0$  limits for different planar transmission lines is finally shown in Table 1. Looking at microstrip and slotline limits it turns out that the range 50  $\Omega$ -100  $\Omega$  would be possible to realize without additional transformers. For low noise pick-ups the losses are very important. Since the microstrip attenuation increases with  $Z_0$  and the slotline losses decrease for higher  $Z_0$  (Fig. 1) an optimum is to be expected around 70  $\Omega$ .

### 3. THEORETICAL MODEL

Consider a charged particle beam (Fig. 8) propagating in +z-direction between two infinite metallic planes at  $x = \pm d$ . The image current density distribution  $\vec{J}_z$  [A/m] may be described as:

$$\vec{J}(x = \pm d) = \vec{u}_z \cdot f(x = \pm d, y, z, t)$$

$\vec{u}_z$  = unit vector in positive z-direction.

A transverse (with respect to the beam) slot (width  $s$ ) of infinite length in  $xy$ -direction in one of the conducting planes (e.g. at  $x = \pm d$ ) could be described in terms of a slotline. This slotline, since it is not (yet) backed by a dielectric material other than vacuum would have a propagation velocity  $v_{slot} = c$  (TEM case). For a slotline on a dielectric substrate, in general a frequency dependent propagation velocity  $v_{slot}(\omega) < c$  would be obtained. In the following considerations it is assumed that  $v_{slot}$ , and also the slotline characteristic impedance  $Z_L$ , are independent of frequency (neglecting the dispersion). Thus each current element  $\vec{J}_z$  would "see" two parallel resistors  $Z_L$  and launch waves in  $xy$ -directions. The voltage across the slotline  $V_s$  then turns out to be:

$$V_s = J_z \cdot dy_0 \cdot Z_L/2 \quad (2)$$

assuming  $J_z$  not to be perturbed by the slot.

As a first approximation we assume that for a single current element at a source point  $x = d, y_0, 0$   $\vec{J}_z$  may be written as:

$$\vec{J}(d, y_0, 0, t) = \delta(y_0) \cdot f(t) \vec{u}_z = g(x=d, y, z, t) \cdot \vec{u}_z \quad (3)$$

Let us remark that:

$$J(d, y_0, 0, t) = J(d, y_0, z, t+z/v_{beam})$$

whatever  $J$  is, an observer at any position  $x = d, y, z = 0, t$  sees:

$$V_s(y, t) = \frac{Z_L}{2} \int_{-\infty}^{+\infty} J \left( y_0, t - \frac{|y - y_0|}{v_{slot}} \right) dy_0 \quad (4)$$

rewritten as:

$$V_s(y, t) = \frac{Z_L}{2} \int_{-\infty}^y dy_0 J \left( y_0, t - \frac{y - y_0}{v_{slot}} \right) + \frac{Z_L}{2} \int_y^{+\infty} dy_0 J \left( y_0, t + \frac{y - y_0}{v_{slot}} \right) \quad (5)$$

With the present assumption the image current distribution  $g(x=\pm d, y, z, t)$  and the transversely ( $\pm y$ ) travelling waves in the slotlines are propagating both with  $v = c$  ( $v_{\text{beam}} = v_{\text{slot}} = c$ ) perpendicular to each other. The observer at  $y$  will measure a voltage across the slotline which has been raised from an image current distribution along the line:

$$y - y_0 = z \cdot v_{\text{slot}}/v_{\text{beam}}$$

(dashed line in Fig. 8 ) for slotline waves in  $+y$  direction and

$$y - y_0 = -z \cdot v_{\text{slot}}/v_{\text{beam}}$$

(dotted line in Fig. 8 ) for slotline waves in  $-y$  direction.

Thus by separating the  $+y$  and  $-y$  travelling slotline waves one obtains at a given time  $t$  the superposition of an image current distribution along a  $\pm 45^\circ$  line (Fig. 8c) if  $v_{\text{beam}} = v_{\text{slot}}$  or more generally:

$$\text{tg}\alpha = \frac{v_{\text{slot}}}{v_{\text{beam}}} \quad (6)$$

Under the further assumption that each surface current element can be attributed only to charged particles travelling perpendicularly above or below it one might interpret the signal  $V_S(y, t)$  as being raised from a particle population in two sample disks of the beam tilted by  $\pm\alpha$  to the  $z$ -axis. Separating the  $+y$  and  $-y$  propagating slotline wave (e.g. by measuring  $V_S(y, t)$  at a distance  $y$  where  $|\vec{J}_z| \approx 0$ ) a pick-up signal corresponding to a single tilted sample disk of the beam can be found.

#### 4. EXPERIMENTAL SLOTLINE PICK-UP STRUCTURES

The first mask, which was used to investigate the properties of a slotline pick-up, is reproduced in Fig. 9a (scale 1). It contains (from left to right) one line with  $Z_L = 150 \Omega$ , 3 lines  $Z_L = 100 \Omega$  and 3 lines  $Z = 50 \Omega$  on a 3 mm alumina substrate. The impedances were calculated for  $f = 1.5$  GHz. Slotline-coaxial cable transition are provided at each end of the slotline, soldering a semirigid cable on the metallized substrate surface with the inner conductor across the slot next to the circle (= open end). For the realisation of all masks shown here, the "MICROS 3" CAD programme<sup>5</sup> has been used. It turned out that already for this very simple approach reasonable electrical properties could be obtained and that this structure is well suited to investigate the mutual coupling between slotlines, effects of mismatches, radiation and attenuation. Figure 11 exhibits the S-parameters for a single  $50 \Omega$  slotline with two transitions to  $0.141''$  semirigid cable. The S-parameter  $S_{11}$  (reflexion coefficient) and  $S_{21}$  or  $S_{12}$  (transmission coefficient) are defined as the complex ratio of the reflected wave/incident wave and transmitted wave/incident wave, respectively. In the frequency range 1-4 GHz the transmission characteristic is reasonably flat and about half the transmission loss (ca 1 dB) can be explained by mismatch (-10 dB). Since the transmission loss  $\alpha$  amounts to roughly 3 dB/m (see Fig. 1), the radiation loss would be below 0.2 dB (2 dB/m). It should be pointed out that the intended

interaction mechanism with the beam is not due to radiation (since slotlines or slots are often used as radiating elements in antenna arrays). It rather works like a transformer, where the image current produces some voltage in a given load.

If more than one slotline is provided, mutual coupling will take place (Fig. 12). Here the behaviour of a directional coupler can easily be recognized. The directivity turns out to be about 10-15 dB (1-4 GHz) and the forward coupling gives a relatively flat response in the same frequency range. A good theoretical treatment of slotline couplers and microstrip couplers can be found in [2] and [7].

For measurements of the pick-up response the field of a beam is simulated by a wire closely mounted ( $= 2$  mm) above a conducting ground plate which forms a  $50 \Omega$  transmission line, where most of the energy is concentrated between the wire and the ground plate. For quantitative calibration reference measurements were carried out with  $50 \Omega$  and  $100 \Omega$   $\lambda/4$  loop (or stripline) pick-ups positioned at the same distance  $h$  ( $h > 10$  mm) from the ground plate as the slotline metallization. Here the structure from Fig. 9b was mainly looked at, because resonant slotlines give a response more similar to loop pick-ups than travelling wave slotlines. The length of these slots in Fig. 9b approaches  $\lambda/2$  at 1.5 GHz,  $Z_0 = 50\Omega$ . For an image current element passing in the middle of that array, each short circuit transforms into an open one at  $\lambda/4$  distance from the short circuit and the entire structure should have an impedance of  $8 \times 50 \Omega$ . Considering a beam close to the surface in the middle of the array, one may assume that nearly all the image current is passing over the slotline at  $y = 0$  (Fig. 8b), thus resulting in a power extraction of  $I_{\text{beam}}^2/4 \times 400 \Omega$  which is equivalent to a beam coupling impedance of  $100 \Omega$  for a single pick-up plate. The results of these measurements (Fig. 13) prove that a single resonant slotline (TSWS) has a pick-up response comparable to a single  $\lambda/4$  loop (centred beam). If the outputs of either side are combined in a 4 to 1 power combiner (proper delay for each output provided), a smoothing effect can be found (Fig. 13b) and slight losses due to the combining network have to be accepted. For an off-centred beam, however, one might obtain deep notches (Fig. 14a) in the response characteristic due to interference effects on the slotline ( $v_{\text{slot}}$  is only 0.5 c). The shape of the curves in Fig. 13 were also confirmed by measurements carried out at Argonne National Laboratory with a 22 MeV electron beam<sup>6</sup>. For these measurements the distance of the beam from the pick-up plate was 15 mm and with the combined signals of the 8 slotlines the maximum coupling impedance was found to be about  $50 \Omega$ . The missing factor 2 (or 3 dB) can be attributed partly to losses in the 8:1 power combiner ( $\approx 1$  dB) and 8 times 2 metre coaxial cable. The other part is due to the fact that not all the image current passes over the centre of the slotline since the beam is already 15 mm apart.

The staggered slotlines ( $100 \Omega$ ) in Fig. 10 have been realized in conjunction with a microstrip combiner board containing Wilkinson power combiners. Microstrip-slotline transitions with a through hole (Fig. 5a) were applied in this case. The distinct ripple and rather poor sensitivity (compared with results for Fig. 9) is a difficulty linked to staggered slotlines. But with an average signal level 6 dB above the response of a single  $\lambda/4$ ,  $100 \Omega$  loop (Fig. 14b : 3 dB loss in the matching resistor ( $50\Omega$  coaxial line -  $100\Omega$  loop))

approximately the same beam coupling impedance per unit length in the frequency range 1-2 GHz as such a loop has been obtained.

## 5. CONCLUSION

The theoretical and measured results on planar slotline pick-ups indicate that these structures might become an interesting alternative to both the well known stripline or  $\lambda/4$  loop pick-ups as well as the slot pick-ups on Faltn type structures.

Present fabrication methods allow very small dimensions in the surface pattern on the alumina substrate. The process involved is relatively easy and returns a very good reproducibility with tight tolerances.

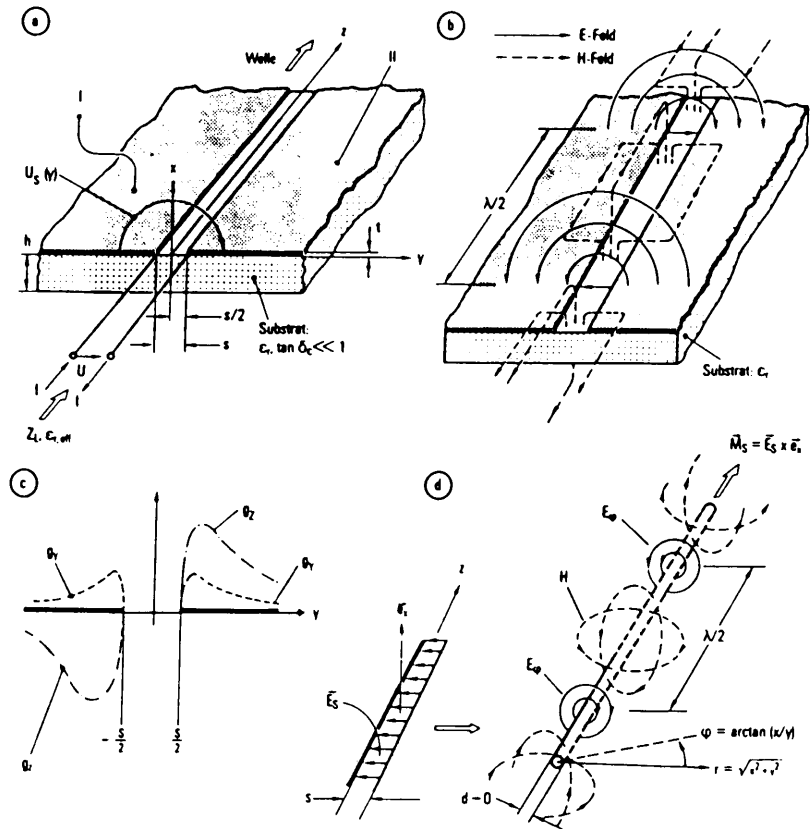
Resonant slotlines (TSWS) could have a higher beam impedance than stripline  $\lambda/4$  loops for a centred beam, but for an offset beam a faster lateral decay in sensitivity should be taken into account. Resistive losses are about comparable to loop pick-ups. Travelling wave slotlines (TTWS) offer the possibility of various sample choices on the beam. For a transverse slotline with  $v(\text{slot}) = c/2$  and a beam ( $v(\text{beam}) = c$ ) the normal vector of the sample disk would be at  $63^\circ$  to the beam axis ( $45^\circ$  for  $v(\text{slot}) = c$ ). By changing the angle of the slotline nearly any angle of the sample disk can be set. This also applies for "slow" beams e.g. heavy ions. Since the slotline must not necessarily be straight a variety of sample disks may be chosen. For a TTWS the beam diameter is not limited to about  $\lambda/2$  at the center frequency since the slotlines interact mainly with the TEM-like wakefield of the beam. Possible waveguide modes in the beampipe may be suppressed by means of absorbing material.

## ACKNOWLEDGEMENTS

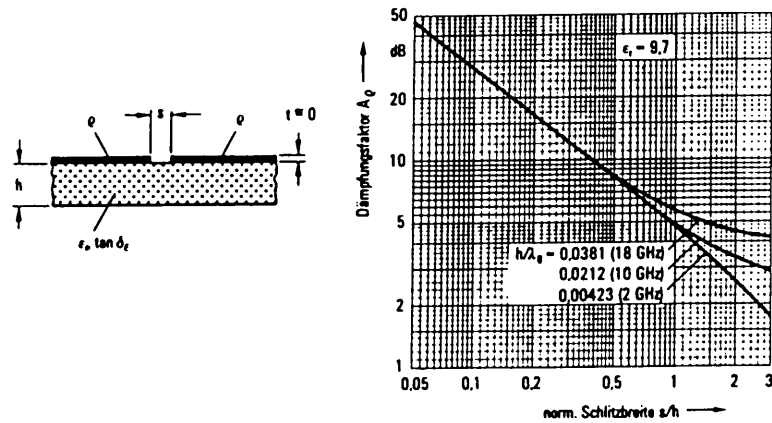
The author would like to thank B. Autin, G. Dôme, L. Thorndahl and S. van der Meer for many valuable discussions and E. Jones for support. All masks have been realized by J.F. Zurcher, EPFL-LEMA (Lausanne) using the MICROS-CAD programme.

## REFERENCES

1. L. Faltn, Slot-Type Pick-up and Kicker for Stochastic Beam Cooling, CERN/ISR-RF/77-47, 1977.
2. R.K. Hoffmann, Integrierte Mikrowellenschaltungen, Springer Verlag 1983.
3. K.C. Gupta, R. Garg and I.J. Bahl, Microstrip Lines and Slotlines, Artech House 1979.
4. F. Caspers, A Broadband Slotline Pick-up, PS/AA/ACOL Note 31, CERN, Feb. 1985.
5. J.F. Zurcher, "MICROS 3" A CAD/CAM Program for Microstrip Circuits EPFL Lausanne-LEMA, 1985.
6. D. Suddeth, Argonne National Laboratory, Private Communication.
7. M. Aikawa and H. Ogawa, A New MIC Magic-T Using Coupled Slotlines, IEEE-MTT-28 No 6, June 1980, pp. 523-528.



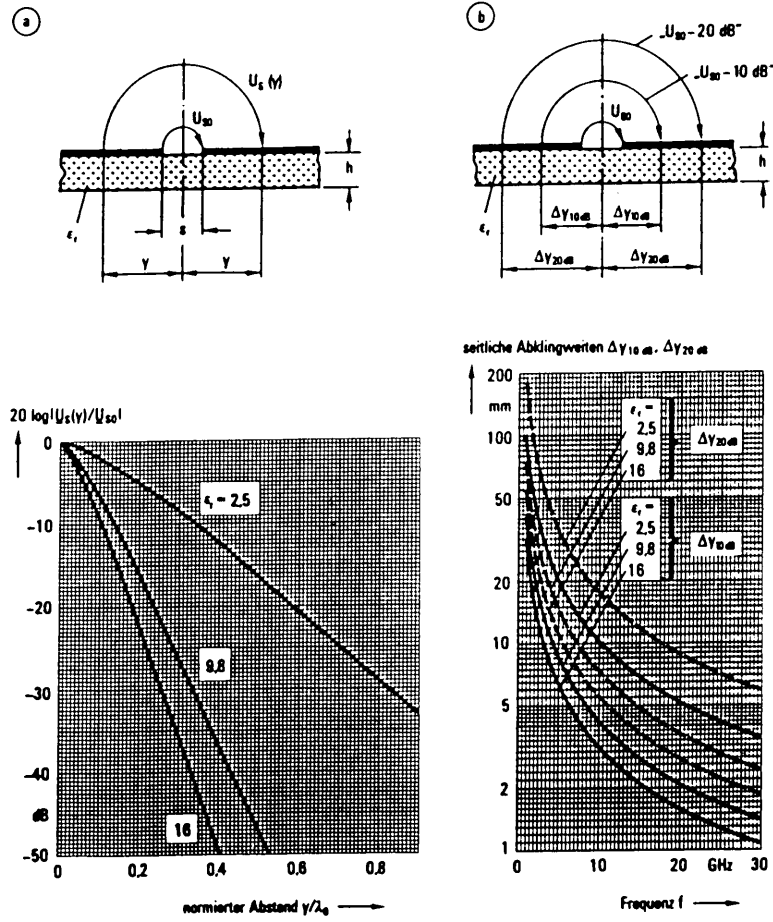
Schlitzleitung. a) Aufbau; b) Feldbild nach TE-Wellennäherung; c) qualitative Verläufe der Längs- und Querstromdichten  $g_z$  und  $g_y$  auf jeweils einer Seite der Elektroden I, II; d) magnetisches Linienstrommodell



Leiterdämpfungsfaktor  $A_p = \alpha_p Z_L h / R_F$  der Schlitzleitung auf  $Al_2O_3$ -Keramiksubstrat ( $\epsilon_r = 9,7$ ) nach /3.140/; Frequenzangaben gelten für  $h = 0,635$  mm.

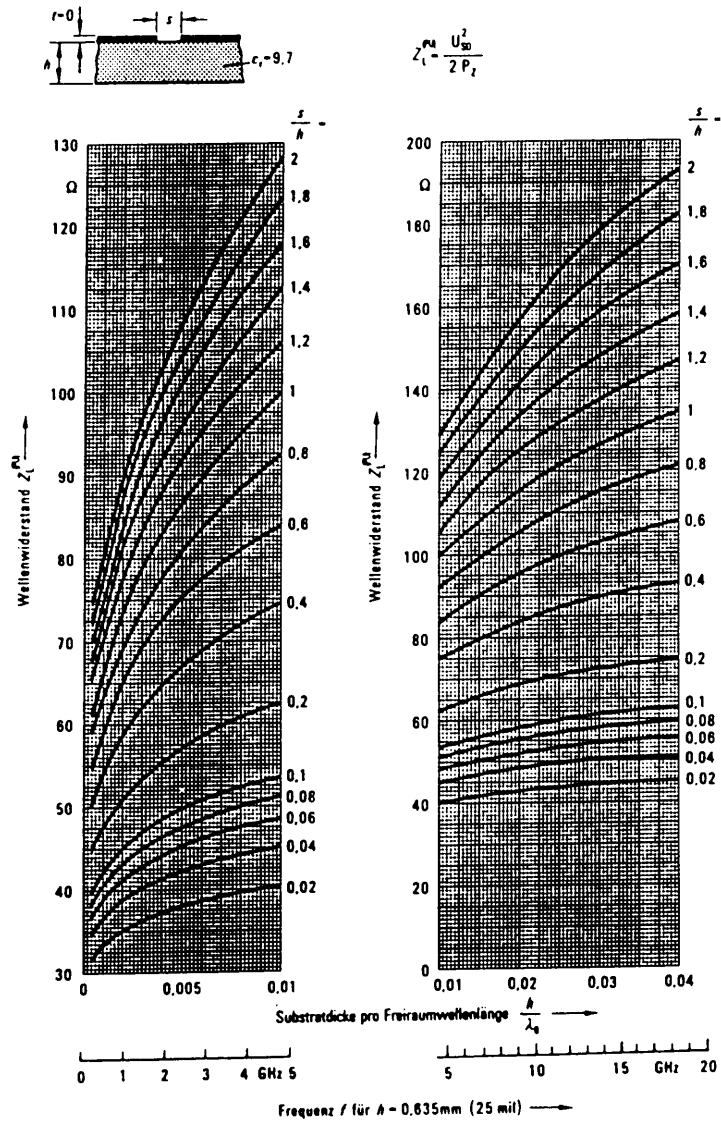
Fig. 1 - Field configuration and losses of slotlines (from [2]).





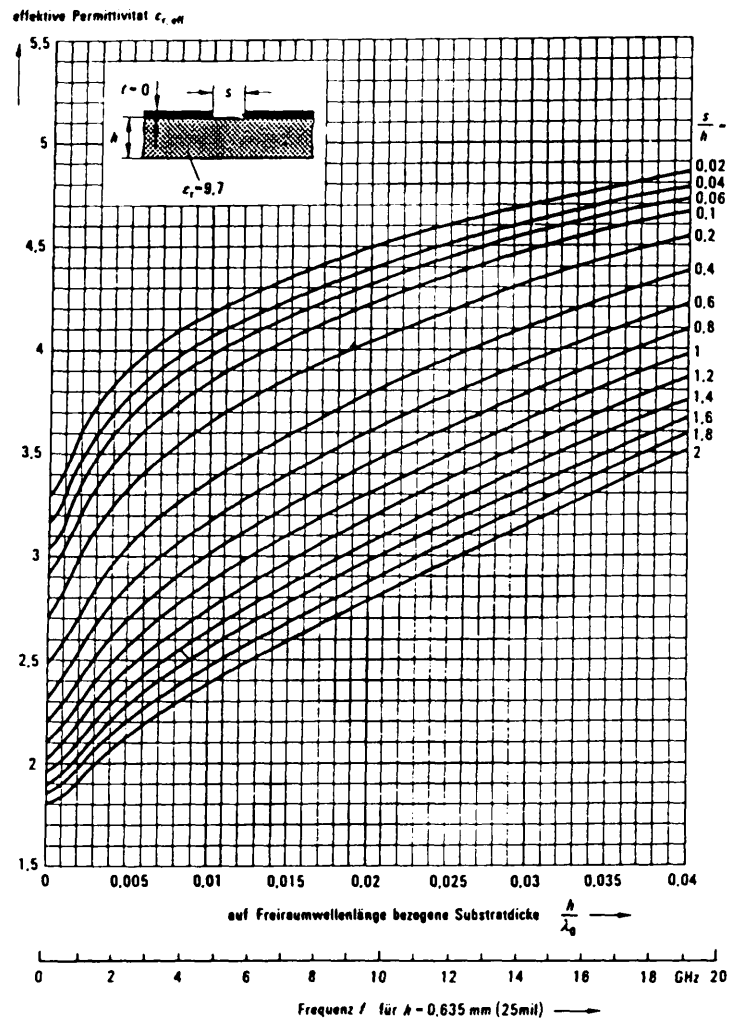
Seitliches Abklingen der Schlitzleitungsspannung in größerer Entfernung vom Schlitz. a) Seitlicher Verlauf der normierten Schlitzleitungsspannung  $U_S(y)/U_{S0}$ ; b) seitliche Abklingweiten  $\Delta y_{10dB}$ ,  $\Delta y_{20dB}$  für einen Spannungsabfall um 10 dB bzw. 20 dB

Fig. 2 - Lateral decay of voltage across the slotline (from [2]).



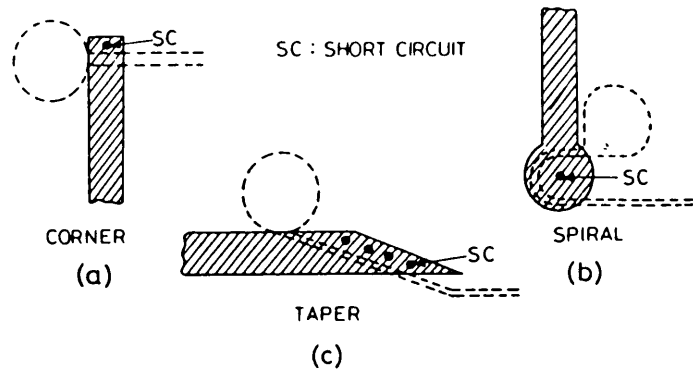
Wellenwiderstand  $Z_L^{(PU)}$  der Schlitzleitung auf  $Al_2O_3$ -Keramiksubstrat ( $\epsilon_r = 9,7$ ) nach der Spannungs-Leistungsdefinition, berechnet nach dem Hohlleiterblendenmodell

Fig. 3 - Characteristic impedance of a slotline (from [2]).

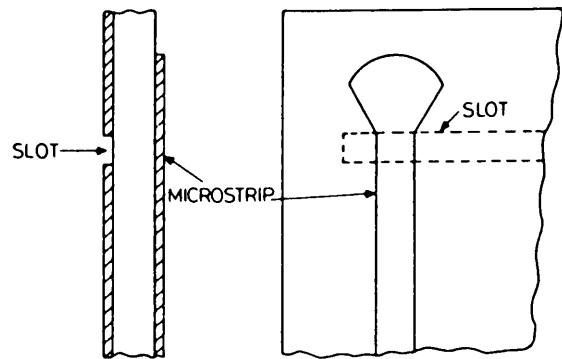


Effektive Permittivität  $\epsilon_{r, \text{eff}}$  der Schlitzleitung auf  $\text{Al}_2\text{O}_3$ -Keramiksubstrat ( $\epsilon_r = 9.7$ ), berechnet nach dem Hohlleiterblendenmodell

Fig. 4 - Effective permittivity of a slotline (from [2]).



*Wide Band Microstrip-Slotline Transitions*



*A Different Type of Microstrip-Slotline Transition*

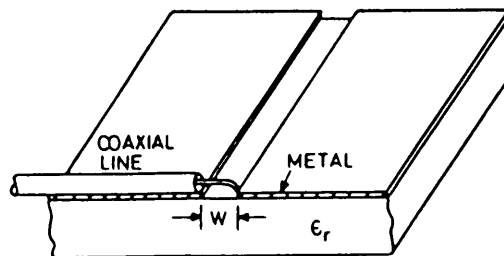
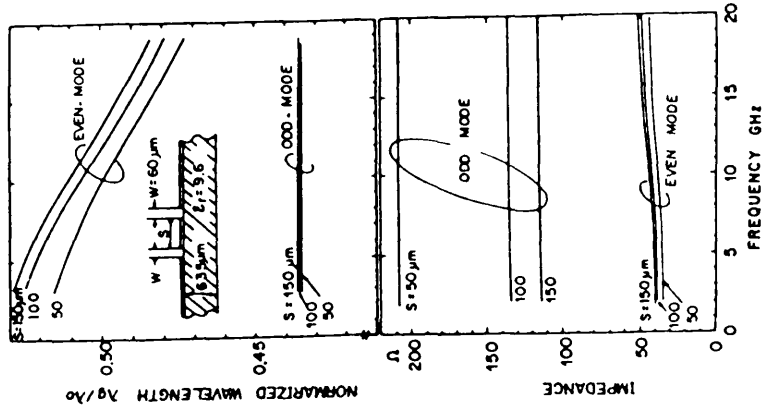
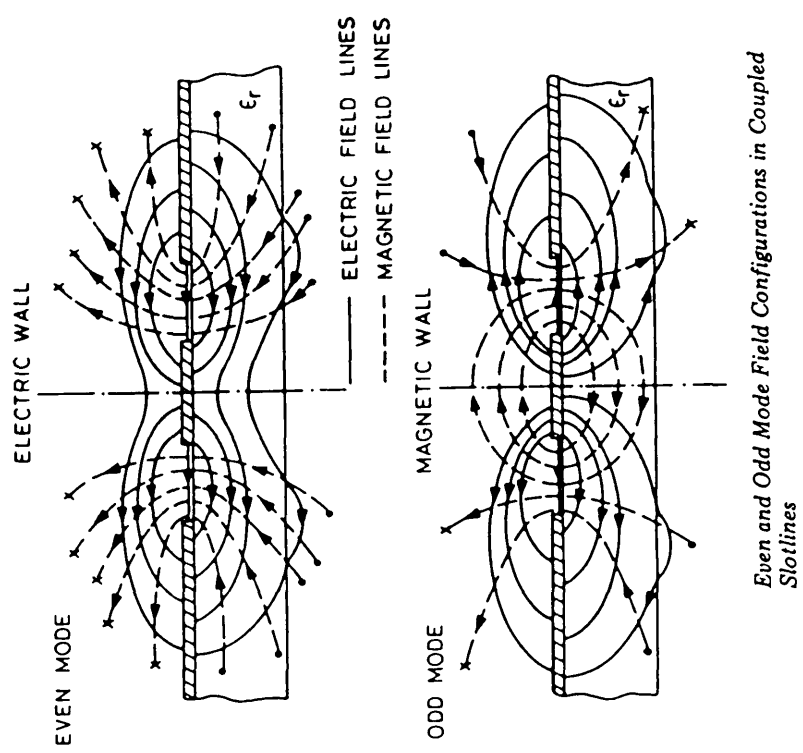


**Fig. 5** - Microstrip-slotline and coaxial slotline transitions (from [2]).



Theoretical characteristic impedance and normalized wave-length of coupled slot lines on a  $\text{Al}_2\text{O}_3$  substrate.

Fig. 6b - Modes on coupled slotlines (from [7])



Even and Odd Mode Field Configurations in Coupled Slotlines

Fig. 6a - Coupled slotlines (from [3])

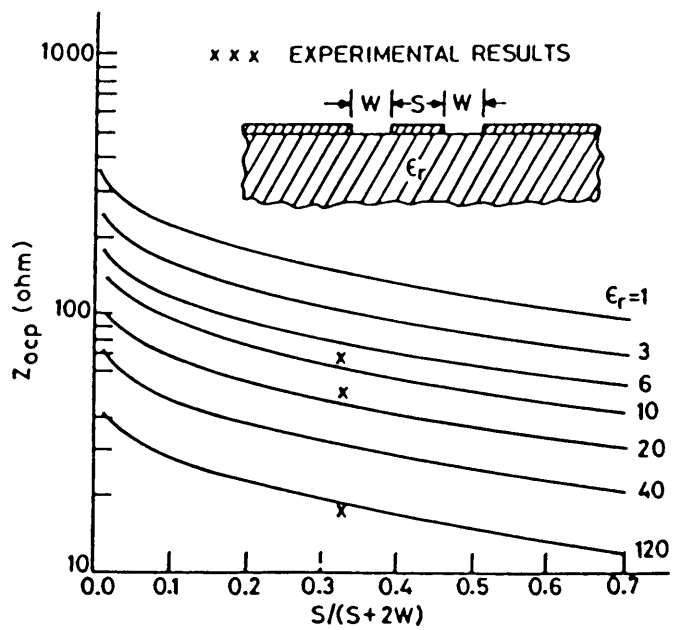
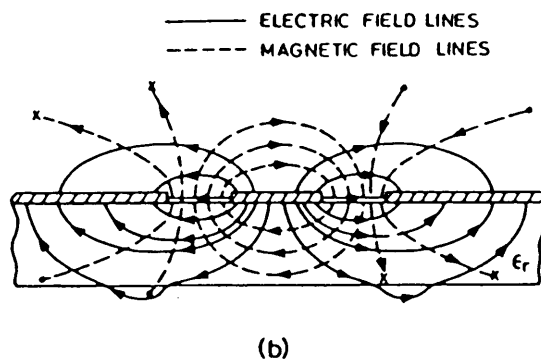
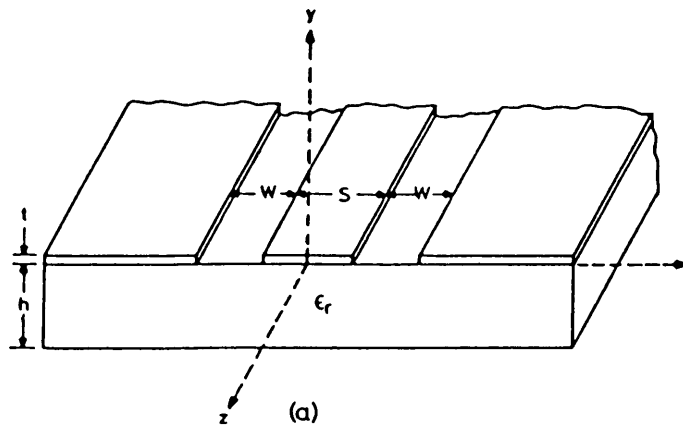


Fig. 7 - Coupled slotlines or coplanar wave guides (from [3]).

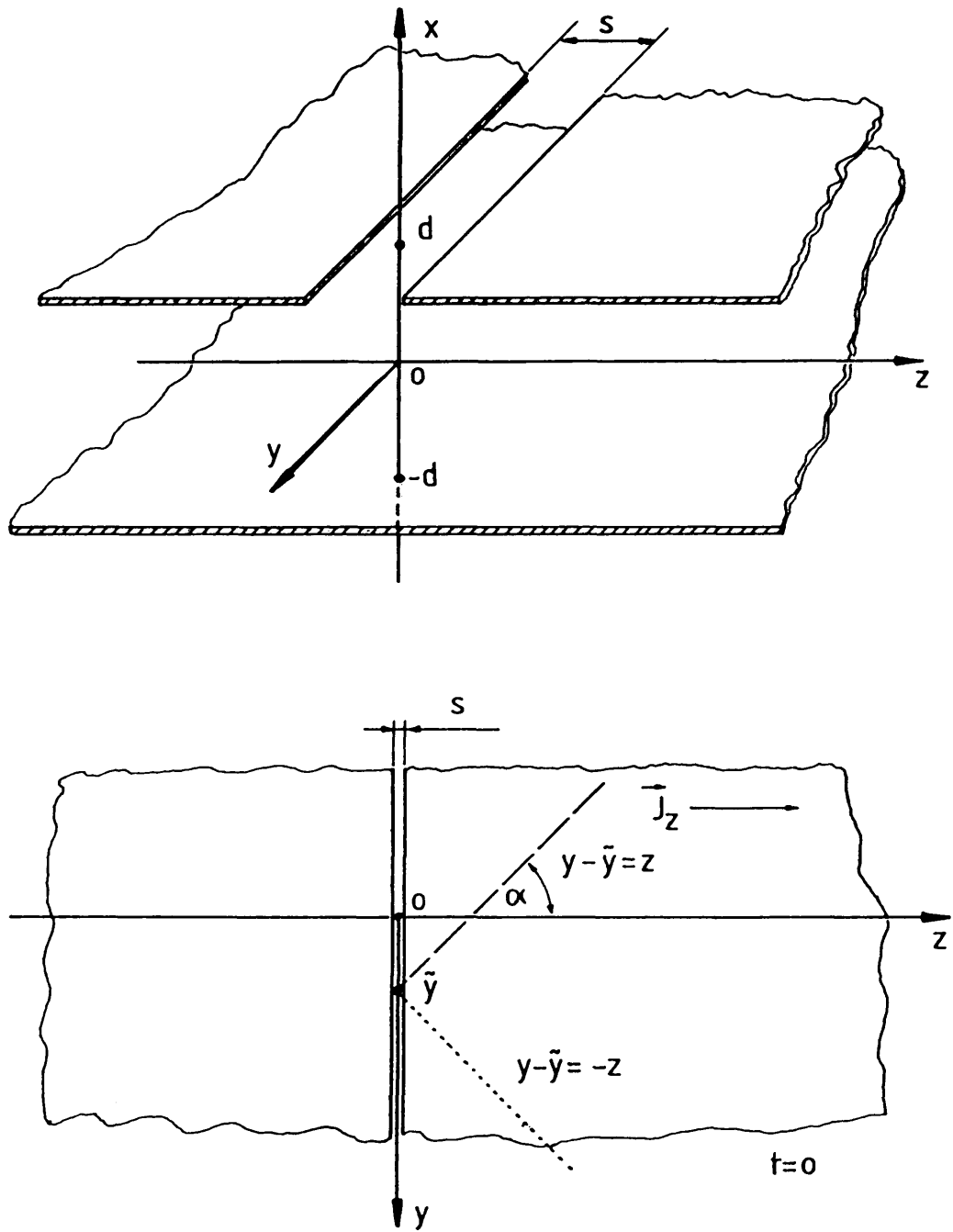
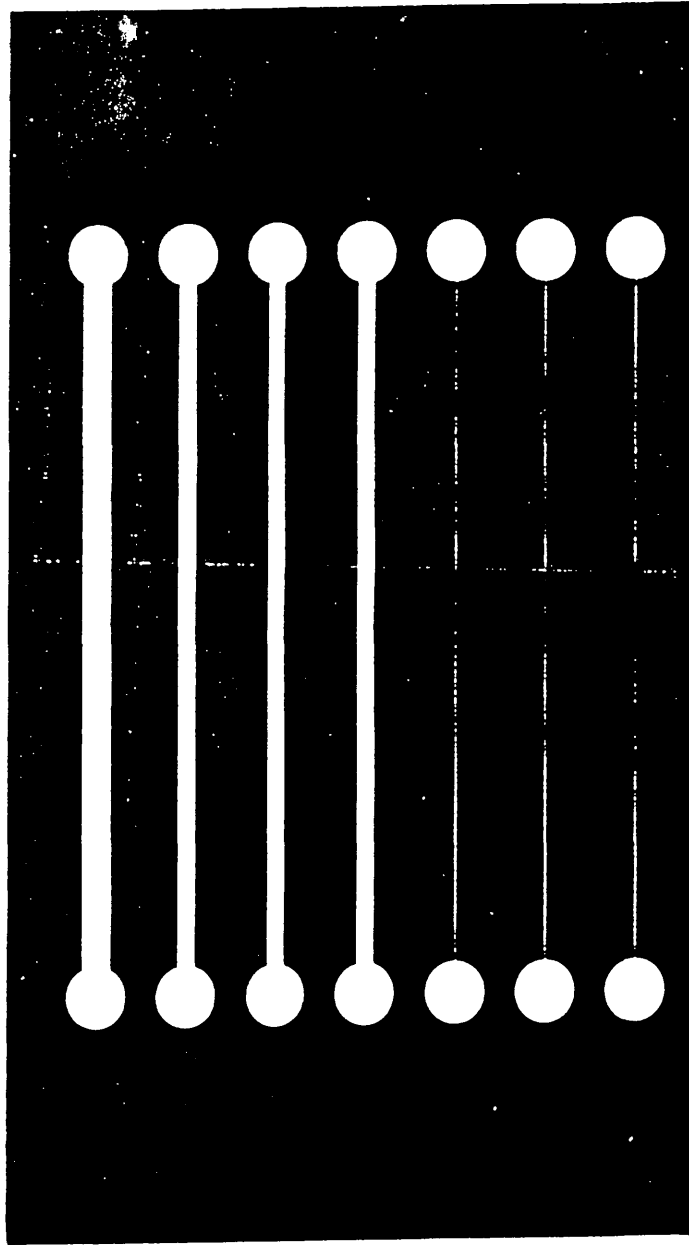


Fig. 8 - Slotline and beam coordinates



100 mm

Fig. 9a - Mask for experimental (transverse travelling wave) slotline pick-up (from [4])



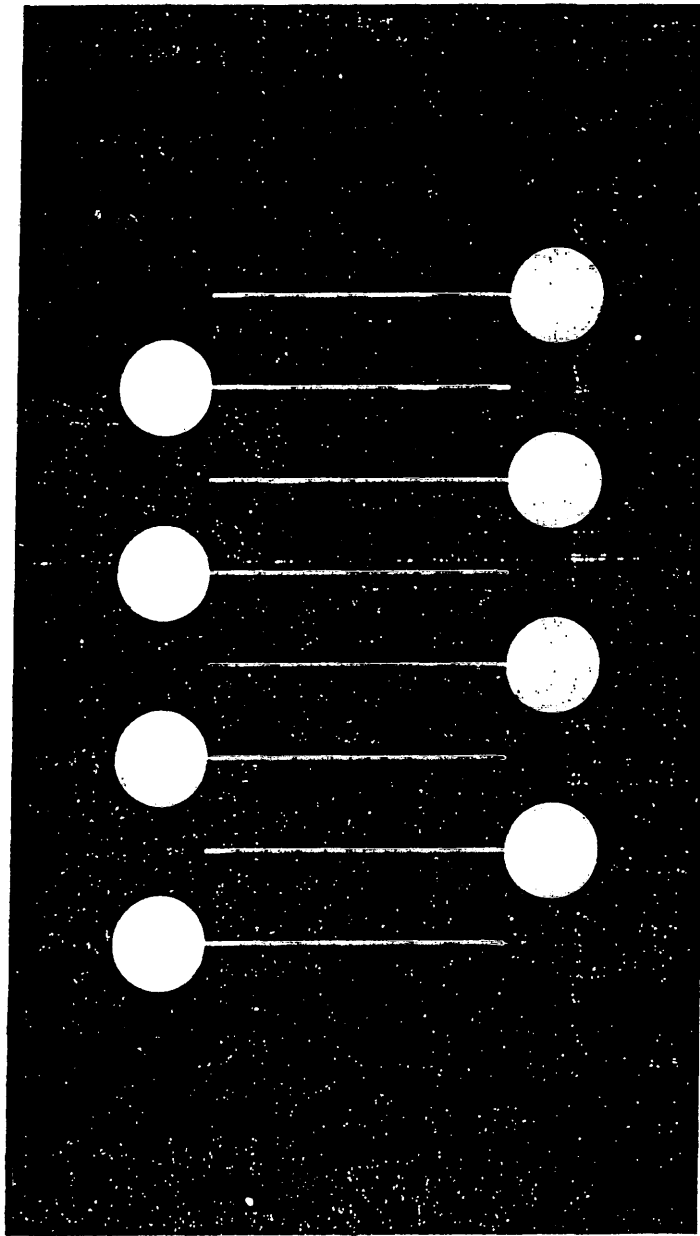


Fig. 9b - Mask for experimental (transverse standing wave) slotline pick-up ( $f_0 = 1.5$  GHz) (from [4])

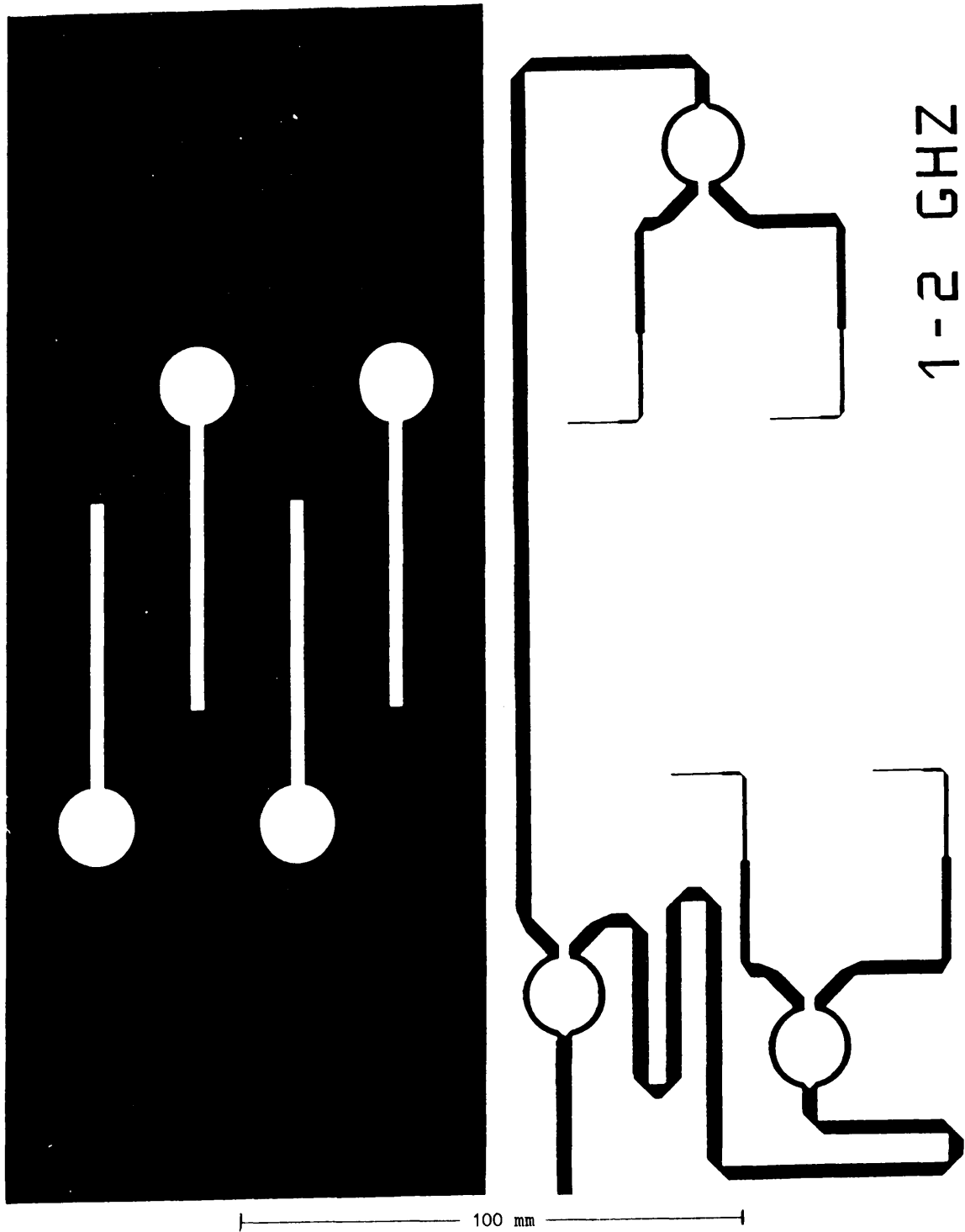


Fig. 10 - Mask for staggered standing wave slotline pick-up ( $4 \times 100 \Omega$ ;  $f_0 = 1.5 \text{ GHz}$ );  
microstrip combiner board (right)

S11            log MAG            S21            log MAG  
REF 0.0 dB            REF 0.0 dB  
10.0 dB/            1.0 dB/

hp

C

START 0.045000000 GHz  
STOP 5.000000000 GHz

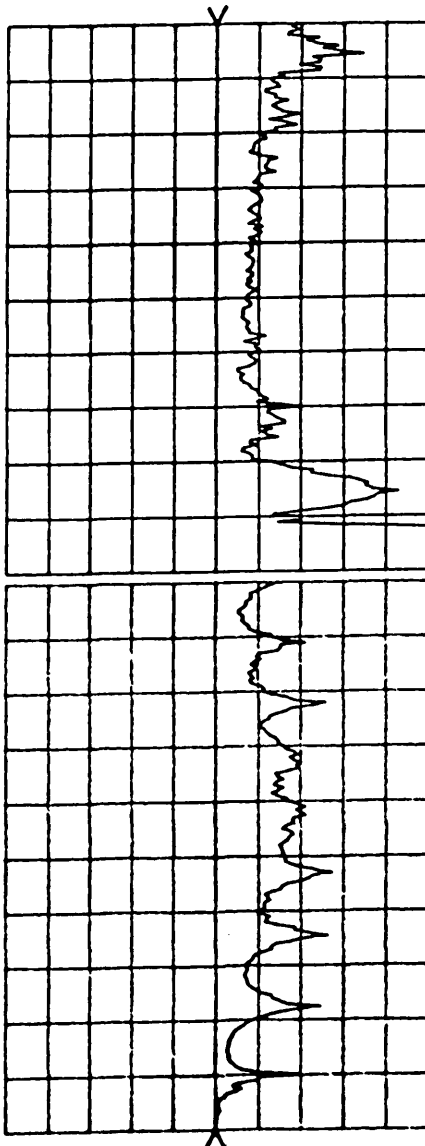


Fig. 11 - Reflexion and transmission of a single 50  $\Omega$  slotline (Fig. 9a) with slotline-semirigid cable transitions; all other slotlines are covered

REF 0.0 dB  
10.0 dB/

log MAG

S21 REF 0.0 dB  
10.0 dB/

log MAG

START 0.045000000 GHz  
STOP 5.000000000 GHz

C

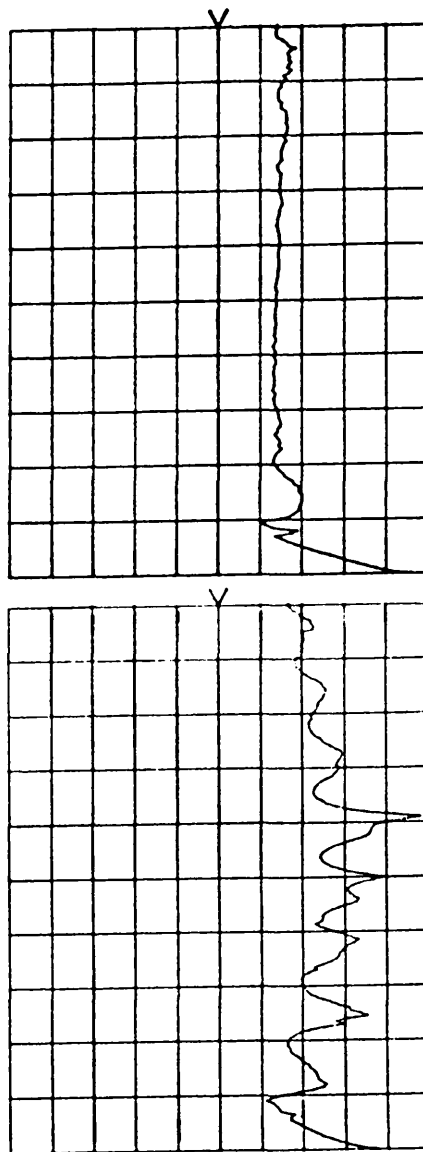


Fig. 12 - Backward (left) and forward coupling (right) between adjacent 50  $\Omega$  slotlines (Fig. 9a)

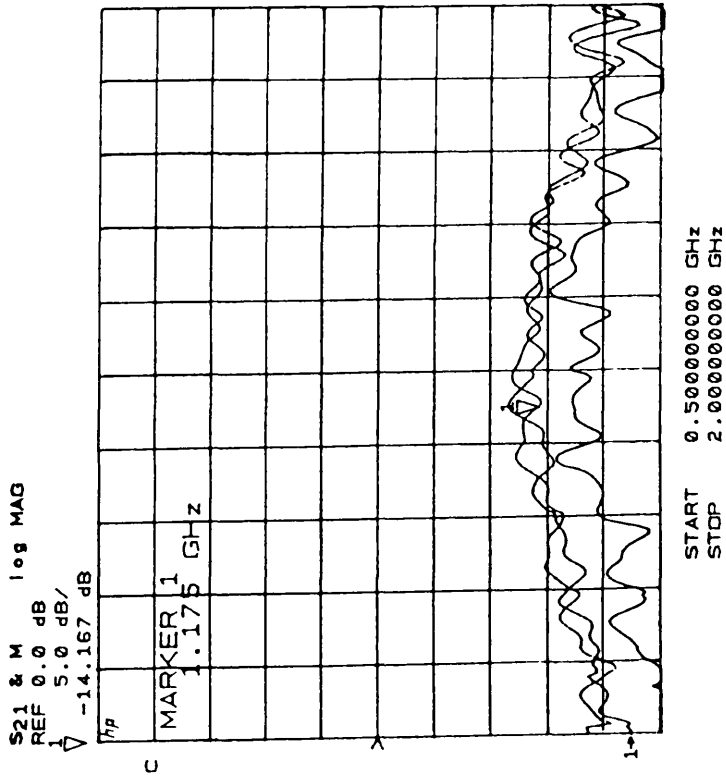


Fig. 13a - Pick-up response of a 50  $\Omega$   $\lambda/4$  loop and a single 50  $\Omega$  resonant slotline (left); simulated beam centred

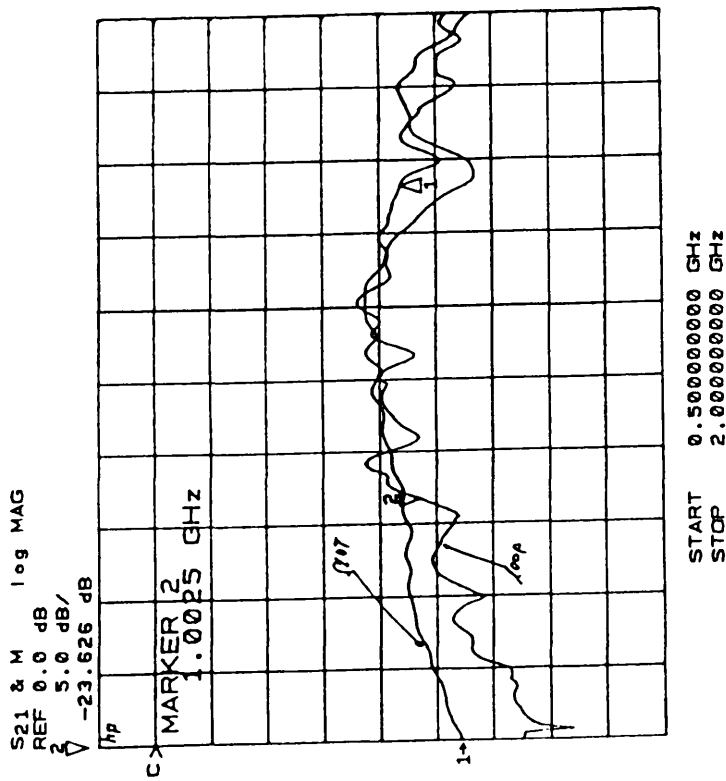


Fig. 13b - Pick-up response of  $\lambda/4$  loop (lower trace) and 4 combined resonant slotlines (Fig. 9b) of either side (upper trace); simulated beam centred

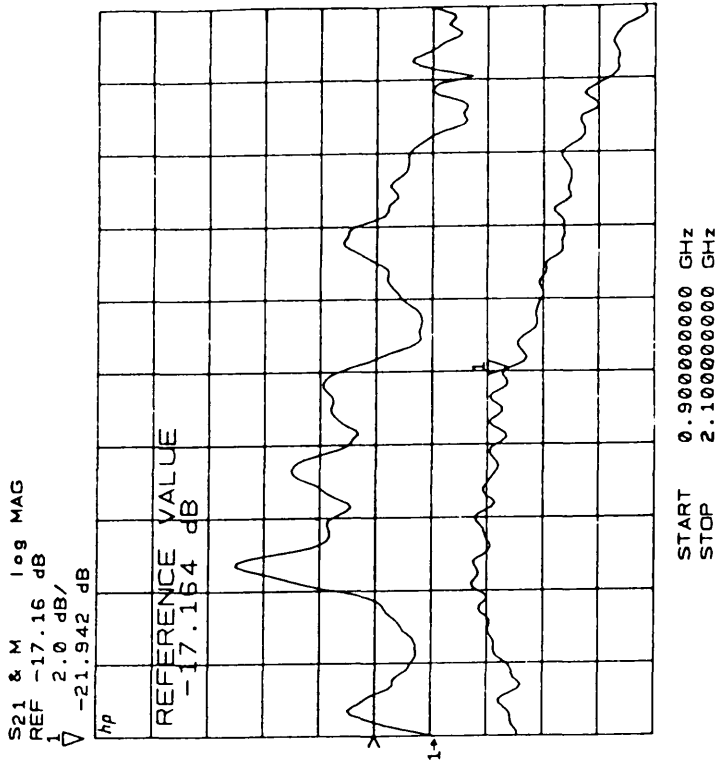


Fig. 14b - Pick-up response of a  $100 \Omega \lambda/4$  loop with matching resistor (lower trace) and the slotline structure (Fig. 10) with combiner board (upper trace); simulated beam centred

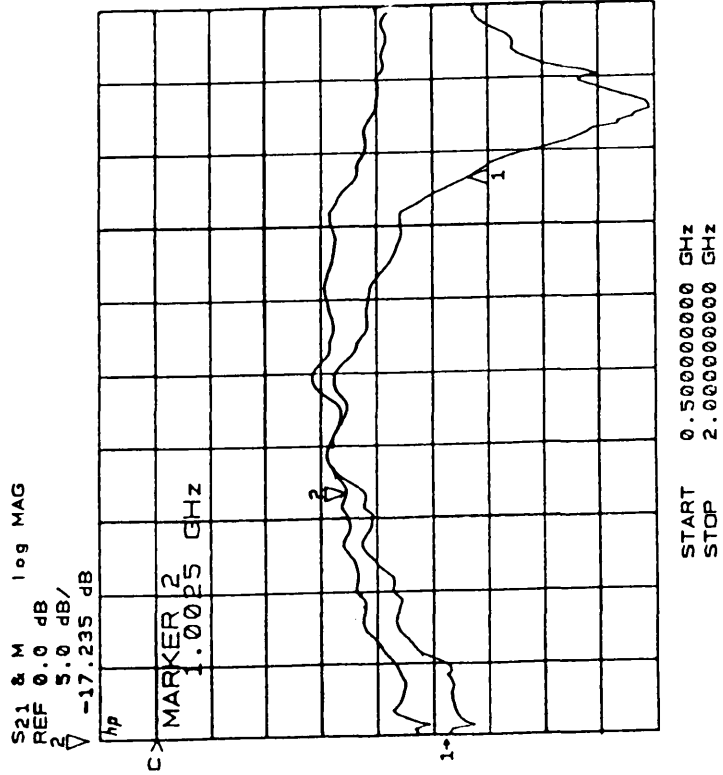


Fig. 14a - Pick-up response of 4 combined resonant slotlines (Fig. 9b) for a centred beam (2) and a beam with 2 cm offset to the output (1)

Transmission Line	Lower limit for $Z_0$ (ohm)	Upper limit for $Z_0$ (ohm)
Microstrip	20 (m)	110 (d)
Slotline	55 (d)	300 (m)
Coplanar waveguide	25 (m, d)	155 (m, d)
Coplanar strips	45 (m, d)	280 (m, d)

*Comparison of  $Z_0$  limits  
( $\epsilon_r = 10.0$ ,  $h = 25$  mil and frequency = 10 GHz)*

Transmission line	Loss (dB/cm)	
	50 ohm	100 ohm
Microstrip	0.04	0.14
Slotline	0.15*	—
Coplanar waveguide ( $h/W=2$ )	0.08	0.28
Coplanar strips ( $h/W=2$ )	0.83	0.13

\* $\epsilon_r = 16$ ,  $Z_0 = 75$  ohm.

*Comparison of loss for  
various lines ( $\epsilon_r = 10.0$ ,  $h = 25$  mil  
and frequency = 10 GHz)*

Table 1 - Comparison of  $Z_0$  limits and loss (from [3]);  
d = limitation by dimensions; m = limitation by modes